

Calculations on negative-parity states in the nuclei of $A = 36-40$

S. T. Hsieh and M. C. Wang

Department of Physics, National Tsing Hua University, Taiwan, Republic of China

D. S. Chuu

Department of Electrophysics, National Chiao-Tung University, Hsinchu, Taiwan, Republic of China

(Received 25 June 1980)

A shell-model calculation of the negative-parity states in the $A = 36-40$ nuclei is presented. The nucleus ^{40}Ca is assumed to be an inert closed core. Active holes are restricted to the $(1d_{3/2}, 2s_{1/2})$ configurations and an active particle is allowed to occupy the $1f_{7/2}$ or $2p_{3/2}$ orbit. The two-body effective interaction is assumed to be the modified surface-delta type. The energy spectra are calculated from a least-squares fit to the experimental data, varying the $T = 0$ and $T = 1$ strengths of particle-hole and hole-hole interactions and the three single-particle level splittings. Spectroscopic factors, $E2$, $E3$, and $M1$ transition rates, and two-body matrix elements are also calculated and compared with the observed values and the previous theoretical results. The validity of the weak-coupling model is also tested.

[NUCLEAR STRUCTURE $A=36-40$, calculated effective interaction, energy spectra, spectroscopic factors and EM transition rates.]

I. INTRODUCTION

For negative-parity states in nuclei with mass numbers $A = 36-40$, only a few calculations have been performed. Most of these assumed an inert closed ^{32}S core with configuration restricted to within the $(1d_{3/2}^n, 1f_{7/2})$ or $(1d_{3/2}^n, 2p_{3/2})$ space.

In this paper, the nuclei with $A = 36-40$ are calculated within the framework of the shell model. The nucleus ^{40}Ca is assumed to be an inert core. In actual calculations, holes are assumed to be distributed in the $1d_{3/2}$ and $2s_{1/2}$ orbitals and one particle in the $1f_{7/2}$ or $2p_{3/2}$ orbital. The extension of the model space is expected to obtain a better systematically theoretical prediction of odd-parity states in this mass region.

The earlier examples of shell-model calculations on levels of odd parity in the region of the $1d_{3/2}$ shell nuclei were performed by Goldstein and Talmi¹ and Pandya² with the restriction that one proton is in the $1d_{3/2}$ shell and one neutron is in the $1f_{7/2}$ shell. Erne³ extended their model space to include an arbitrary number of nucleons in the $1d_{3/2}$ shell with all inner shells considered an inert ^{32}S core. Twelve two-body interaction matrix elements of the extra-core nucleons and two binding energies to the core were treated as free parameters to fit sixty nuclear levels, including even-parity states belonging to configurations in the $1d_{3/2}$ shell only, of nuclei in the range $^{33}\text{S}-^{41}\text{Ca}$. Under this severely restricted $(1d_{3/2}^n, 1f_{7/2})$ configuration, the agreements between the theoretical and experimental odd-parity levels are, of course, only possible for the very lowest states. Maripuu

and Hokken⁴ studied the nuclei of $A = 35, 37$, and 39 with residual interaction in the form of a modified surface-delta interaction (MSDI). Taking into account the configurations of $(1d_{3/2}^n, 1f_{7/2})$ and $(1d_{3/2}^n, 2p_{3/2})$, great disagreement with the experiment still arose. Neither the energies nor the level order of the identified states of some nuclei could be reproduced well by his calculations. Maripuu *et al.*⁵ calculated energies and wave functions for ^{38}Cl , ^{39}K , and ^{40}K in a model space which included $d_{5/2}$, $s_{1/2}$, $d_{3/2}$, $f_{7/2}$, and $p_{3/2}$ orbitals. The two-body matrix elements used in their Hamiltonian were calculated from the Sussex relative oscillator matrix elements with space truncation effects added. In their calculation, the observed anomalously large $3_2^- \rightarrow 4_1^-$ $M1$ transition strength, which cannot be understood when only assuming a weak-configuration mixing, thus can be correctly predicted. The odd-parity states of nuclei with mass numbers $A = 39-41$ have also been studied by Hsieh *et al.*⁶ They included the complete $2s, 1d$ and $1f, 2p$ shells in a first order Tamm-Dancoff calculation. The spectroscopic factors and EM transition rates were obtained in reasonable agreement with the experimental data. Recently, Hasper⁷ presented a shell-model calculation on even- and odd-parity states of nuclei in the mass region $A = 36-39$. In spite of having used about the same model space (the restriction of the number of nucleons distributed in the $2s_{1/2}$ and $1f_{7/2}$ are different) as has been used in the present work, an inert closed ^{28}Si core was assumed in his work. In addition to this, only seventeen experimental levels were included in his least-squares fit. However,

the reliable experimental data available now certainly include much more than this value. Furthermore, he did not calculate the spectroscopic factors and EM transition and thus there is no way to determine how good the wave functions are.

In this work, we calculate the negative-parity states in $A=36-40$ nuclei assuming the nucleus ^{40}Ca to be an inert closed core. The model assumptions used in the present work are described in detail in Sec. II. Section III gives the results. Conclusions are presented in the final section.

II. ASSUMPTIONS

As indicated above, ^{40}Ca is assumed to be an inert core. One active particle is allowed in the $1f_{7/2}$ or $2p_{3/2}$ orbital while active holes are distributed in the $1d_{3/2}$ and $2s_{1/2}$ shells. The neglect of the $2p_{1/2}$ orbit is, we feel, the most serious constraint on our model. The omission of the $1d_{5/2}$ and $1f_{5/2}$ orbitals from the model space is quite reasonable because the splittings of observed single-particle levels of $2s_{1/2}-1d_{5/2}$ and $1f_{5/2}-2p_{3/2}$ are much larger than those of $1d_{3/2}-2s_{1/2}$ and $2p_{3/2}-1f_{7/2}$.⁸ Since the spacing between $1f_{7/2}-1d_{3/2}$ is comparatively larger than that between $1d_{3/2}-2s_{1/2}$, it is reasonable to assume that only one particle is distributed in the $1f_{7/2}$ or $2p_{3/2}$ active orbital. Under these assumptions, the wave functions of eigenstates can be written as linear combinations of basis states of the form

$$\psi = | [s_{1/2}^{\pi_1} \alpha_1 T_1 J_1, d_{3/2}^{\pi_2} \alpha_2 T_2 J_2] T_h J_h, j_p > T, J, \rangle$$

where $j_p = 1f_{7/2}$ or $2p_{3/2}$.

The Hamiltonian in this space has the form

$$H = H_{hp} + H_{hh} + H_0.$$

Here H_{hp} represents the effective two-body interaction between the particle in the $1f_{7/2}$ or $2p_{3/2}$ orbital and the holes in the $1d_{3/2}$ and $2s_{1/2}$ orbitals. The term H_{hh} represents the two-body effective interaction between the holes in the $1d_{3/2}$ and $2s_{1/2}$ orbitals. H_0 represents single-particle energies for active orbitals which were chosen initially to roughly approximate the observed single-particle spectra of the masses 39, 40, and 41. The initial splitting between single-particle levels was taken from Gerace and Green,⁹ who treated ground-state correlation energy in ^{40}Ca explicitly.

In this study, the two-body residual interactions between particle-hole and hole-hole are assumed to be of the modified surface δ type

$$V_{ij} = 4\pi A_T \delta(\Omega_{ij}) + B_T,$$

where A_0, A_1 are the corresponding interaction strengths for $T=0, T=1$ states, and B_0, B_1 are the corrected terms to the diagonal matrix ele-

ments for $T=0, T=1$, respectively. Four interaction strengths $A_{0ph}, A_{1hp}, A_{0hh},$ and A_{1hh} , four parameters $B_{0hp}, B_{1hp}, B_{0hh},$ and B_{1hh} , and three splittings of single-particle levels of $d_{3/2}-s_{1/2}, f_{7/2}-d_{3/2},$ and $p_{3/2}-d_{3/2}$ were allowed to vary in a least-squares fit to the observed energy spectra. For the selection of energy data, in principle we included all the available low-lying states with reliable J^π assignments up to the point that the first level with uncertain J^π assignment appeared. Exceptions will be discussed individually. Thus a total of 56 experimental energy levels were included in the least-squares calculation to determine the eleven parameters mentioned above. The overall root-mean-square deviation is 0.30 MeV.

III. RESULTS

A. Energy levels

The excitation energies of the negative-parity states were made to fit the observed energy spacing relative to the ground states of nuclei with $A=36-40$. The ground-state energy is defined as

$$E_g = - \{ [E_B(N, Z) - E_B(^{40}\text{Ca})] - (40 - N - Z)[E_B(^{39}\text{Ca}) - E_B(^{40}\text{Ca})] \},$$

where N and Z are the total numbers of neutrons and protons in the nucleus. The calculated interaction strengths for H_{hh} were used to reproduce the even-parity states. In the calculation of ground states, only h-h interactions are considered. Since only the energy spacings relative to the ground states are concerned in our calculation, it is hoped that the adjustable single particle energy may absorb the discrepancy due to the lack of 2p-2h interaction. Table I presents the calculated and observed binding energies of the ground states, with the nucleus ^{40}Ca assumed to be a core. The calculated excitation spectra together with the observed ones for nuclei with $A=36-40$ are shown

TABLE I. Experimental and calculated binding energies of the ground states E_g in MeV by assuming ^{40}Ca as a core.

Nucleus	T	J^π	E_{theo} (MeV)	E_{exp} (MeV)
^{38}K	0	3^+	-2.33	-2.57
^{38}Ar	1	0^+	-1.84	-2.44
^{37}K	$\frac{1}{2}$	$\frac{3}{2}^+$	-6.39	-6.15
^{37}Cl	$\frac{3}{2}$	$\frac{3}{2}^+$	-1.08	-1.09
^{36}Ar	0	0^+	-13.10	-13.09
^{36}Cl	1	2^+	-7.12	-6.41
^{36}S	2	0^+	-2.15	-2.16

in Figs. 1-5. Experimental data are taken from Endt and Leun¹⁰ and Baumann *et al.*¹¹ Levels with an asterisk are included in the least-squares fit.

A first calculation reproduced quite well the level sequence in the individual masses. It, however, exhibited a consistent shift of the ⁴⁰Ca spectrum by about 600 keV to lower excitation energies. This is due to the fact that ⁴⁰Ca is not a very good closed shell. To remove this discrepancy we considered the effect of ground-state correlations to our model calculation. Since the ground-state correlations are stronger in ⁴⁰Ca,¹² we added 0.6 MeV to the gap parameter for ⁴⁰Ca. Thus, the gap for ⁴⁰Ca turned out to be 0.6 MeV larger than the others. This is in agreement with the results of Hsieh *et al.*⁶ and Hubbard and Jolly.¹³

The energy spectra of odd-parity levels for $A = 40$ nuclei are presented in Fig. 1. The agreements between the calculated and the observed energies are reasonably good for most of the levels, especially the 5_1^- and 3_2^- for $T=0$ and the 4_1^- , 3_1^- , 2_1^- , and 2_2^- for $T=1$. In our calculation, the first 1^-

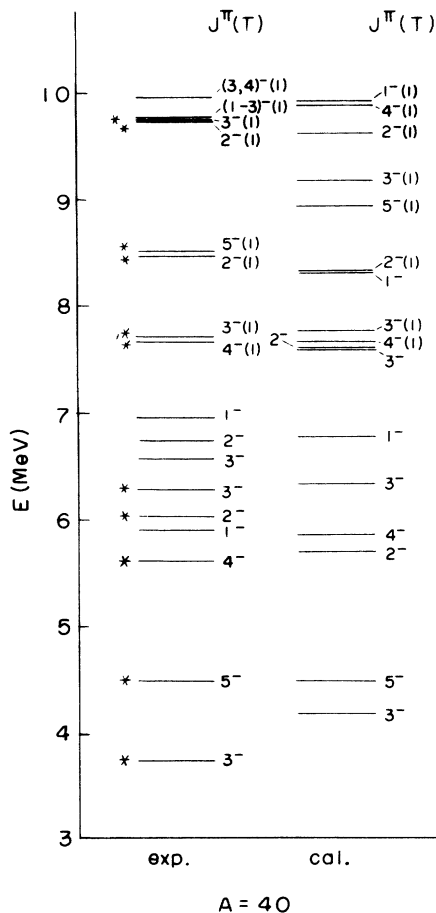


FIG. 1. Experimental and theoretical energy spectra for the $A=40$ nuclei.

state was not included in the fitting and the agreement between the calculated and the observed values for this state is unsatisfactory. The reason for the large discrepancy can be seen from the earlier shell-model calculation by Hsieh *et al.*⁶ Their results showed that the wave function of the 1_1^- state is composed of only 30% of the $(p_{3/2}, d_{3/2}^{-1})$ and $(p_{3/2}, s_{3/2}^{-1})$ configurations, and the triangular rule forbids the $(f_{7/2}, d_{3/2}^{-1})$ or $(f_{7/2}, s_{1/2}^{-1})$ to be the component of the 1^- state. In addition, the effect due to the spurious state on the 1^- state of ⁴⁰Ca is rather large. Therefore, it is beyond the model space considered in this work and has to be excluded in the least-squares fit. The wave functions of the first level for most of J^- for $T=0$ and $T=1$ are almost the pure states of $(f_{7/2}, d_{3/2}^{-1})$ with an intensity larger than 86%. One important point that has to be mentioned here is that even for the lowest lying state, e.g., 3_1^- , the intensities of $(f_{7/2}, s_{1/2}^{-1})$ and $(p_{3/2}, d_{3/2}^{-1})$ are still important and cannot be neglected. This seems to justify the necessity of the inclusion of the $s_{1/2}$ and $p_{3/2}$ configuration space at least.

The calculated and observed energy spectra for $A=39$ nuclei are presented in Fig. 2. Our calculation reproduced quite well the level sequence and most of the level spacings for the nuclei in this mass number. The level at 8.89 MeV was tentatively assigned as $J^\pi = (\frac{5}{2}^-, \frac{3}{2}^-)$, $T = \frac{3}{2}$ (Ref. 14); the fitted $\frac{3}{2}^-$ state at 8.77 MeV favors a J^π of $\frac{3}{2}^-$. Sugarbaker *et al.*¹⁵ investigated the low-lying high-spin states in ³⁹K by using the ⁴¹Ca(d, α)³⁹K reaction. In order to reproduce both the ⁴¹Ca(d, α)³⁹K and ³⁹K(α, α')³⁹K reaction data, they concluded that the spin assignment for the 5.72 MeV level in ³⁹K has to be a J^π of $\frac{13}{2}^-$. Our calculated $\frac{13}{2}^-$ state at 6.01 MeV gives strong support to their suggestion. The importance of the component $(f_{7/2}, d_{3/2}^{-2})$ contained in the wave functions for the yrast states in this mass number decreases appreciably. The intensities of the components $(f_{7/2}, d_{3/2}^{-1}, s_{3/2}^{-1})$, $(p_{3/2}, d_{3/2}^{-2})$, and $(p_{3/2}, d_{3/2}^{-1}, s_{1/2}^{-1})$ for the energy levels in this mass number increase appreciably compared with those for $A=40$. This fact manifests again the necessity of enlarging the model space.

Figure 3 shows the calculated and observed energy levels for the nuclei with $A=38$. The level sequence and spacing are reproduced well. The states at 3.42, 12.32, and 12.42 MeV are uncertainly assigned at $J^\pi = (4, 5, 6)^-$ for $T=0$, and $J^\pi = (1, 2, 3)^-$ and $(2, 3, 4)^-$ for $T=2$ states, respectively. Our calculated 6^- , $T=0$ state at 3.49 MeV seems to favor a 6^- state at 3.42 MeV. The calculated 1^- , $T=2$ state at 12.29 MeV strongly manifests that the state at 12.32 MeV is a 1^- state. The observed level at 12.42 MeV has a theoretical counterpart at 12.71 MeV with $J^\pi = 4^-$ and $T=2$.

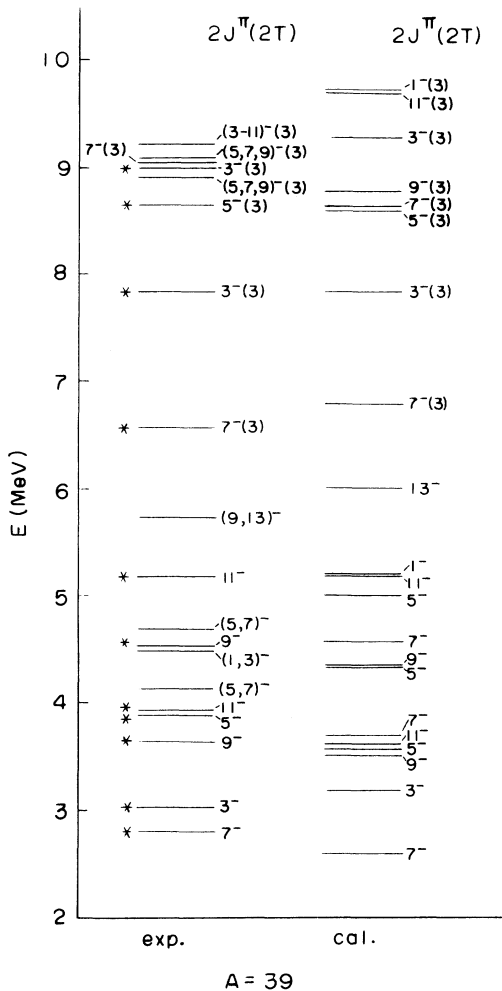


FIG. 2. Experimental and theoretical energy spectra for the $A=39$ nuclei.

Aarts *et al.*¹⁶ studied the high-spin states of ^{38}Ar with the $^{35}\text{Cl}(\alpha, p\gamma)^{38}\text{Ar}$ reaction. Unambiguous spin-parity assignments of $J^\pi=7^-$, 9^- , and 11^- to the ^{38}Ar levels at 7.51, 10.17, and 11.61 MeV were obtained. The levels of 9^- and 11^- are beyond our model space, and the calculated $J^\pi=7^-$ level at 8.49 MeV does not agree as well as the other states. This discrepancy may be improved by enlarging the model space. Most of the states in this mass number have rather strong mixing. There are only a few states with a nearly pure ($f_{7/2}, d_{3/2}^{-3}$) configuration.

Figure 4 presents the experimental and calculated energy spectra for the nuclei with $A=37$. Owing to the severe lack of definite spin assignments, we only calculated the energy levels lying below 4.7 MeV for $T=\frac{1}{2}$. Below this energy, all calculated states have counterparts in the experimental level scheme. Most of the levels included in the

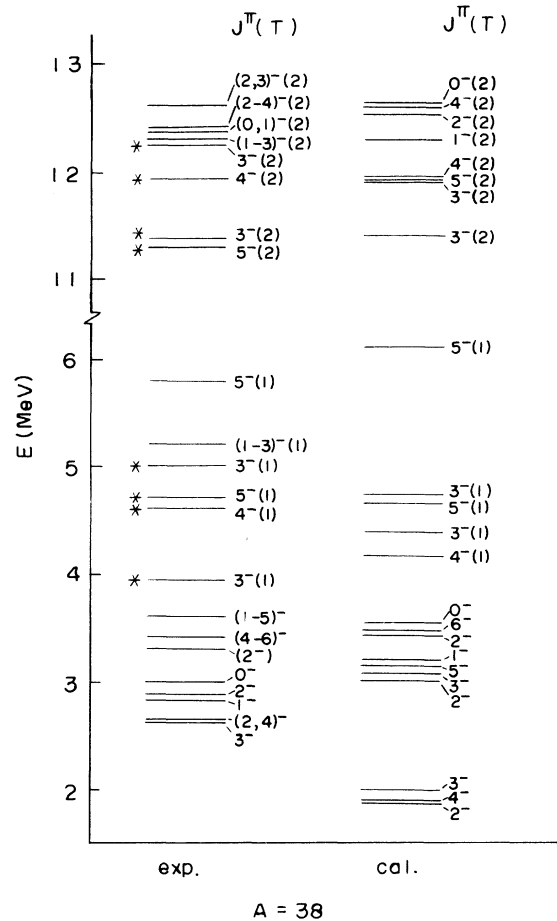


FIG. 3. Experimental and theoretical energy spectra for the $A=38$ nuclei.

least-squares fit agree very well with the observed ones except for the $\frac{3}{2}_2^-, T=\frac{1}{2}$ state, which shifts from the observed value of 3.52 MeV with a large discrepancy of 0.53 MeV. The energy levels excluded in the least-squares fit are also not reproduced well. However, the calculated $\frac{3}{2}^-, T=\frac{1}{2}$ state at 4.63 MeV and $\frac{11}{2}^-, T=\frac{3}{2}$ state at 9.54 MeV are in excellent agreement with the experimental counterparts. Baumann *et al.*¹¹ studied the deexcitation of high-spin states in ^{37}Cl via the $^{27}\text{Al}(^{19}\text{F}, 2p)$, $^{27}\text{Al}(^{12}\text{C}, 2p)$, and $^{34}\text{S}(\alpha, p)$ reactions. A new yrast level at 7.02 MeV with $J^\pi=\frac{15}{2}^-$ was determined from a recoil distance experiment. Our theoretical counterpart for this state is calculated at 8.39 MeV. The reason for this discrepancy may be the restriction of our model space. The mixings of most of the levels for this mass number are stronger than those for the $A=38-40$ nuclei.

The calculated and observed energy spectra for the $A=36$ nuclei are presented in Fig. 5. The fit-

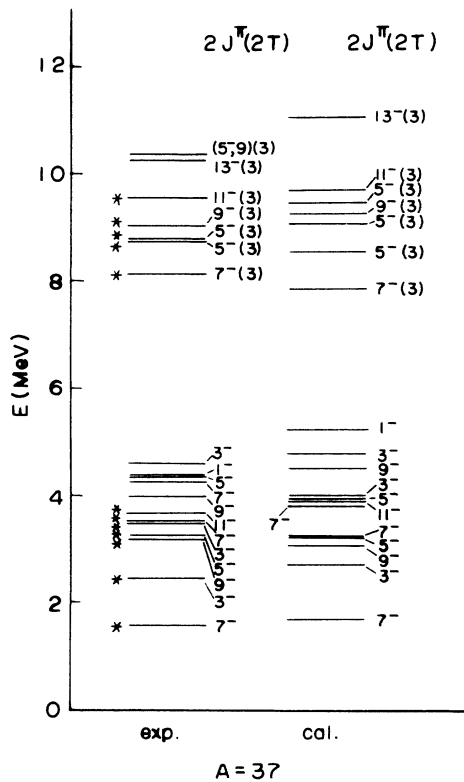


FIG. 4. Experimental and theoretical energy spectra for the $A=37$ nuclei.

ting for this mass number is worse than the others. One level for which the agreement is not good is the first excited 2^- level at 4.97 MeV. The calculated energy spacing value gives a large discrepancy of 0.78 MeV compared to the observed one. In fact, the fit to this state is the worst of all the fittings. The mixings of different components for the energy levels are strongest among the nuclei considered in this work.

In conclusion, our calculated energy levels agree, in general, reasonably well with the observed ones for either the level spacings or the level sequences. The importance of the $s_{1/2}$ and the $p_{3/2}$ orbits is manifested in the large intensities comprised in the $(f_{7/2}, s_{1/2}^{\pi_1}, d_{3/2}^{\pi_2})$ and $(p_{3/2}, s_{1/2}^{\pi_1}, d_{3/2}^{\pi_2})$ components. The intensity of the configuration with $n_1 \geq 3$ for the $s_{1/2}$ orbit is less than 10% for all levels. The mixing between different components increases as the mass number A decreases. For even-mass nuclei, the root-mean-square deviation for each mass number decreases as the mass number A increases. The same conclusion is obtained for odd-mass nuclei. The rms for individual mass numbers $A=36-40$ are 0.403, 0.251, 0.346, 0.204, and 0.280 MeV, respectively. For individual mass numbers, higher isospin states, in general, give a smaller root-mean-

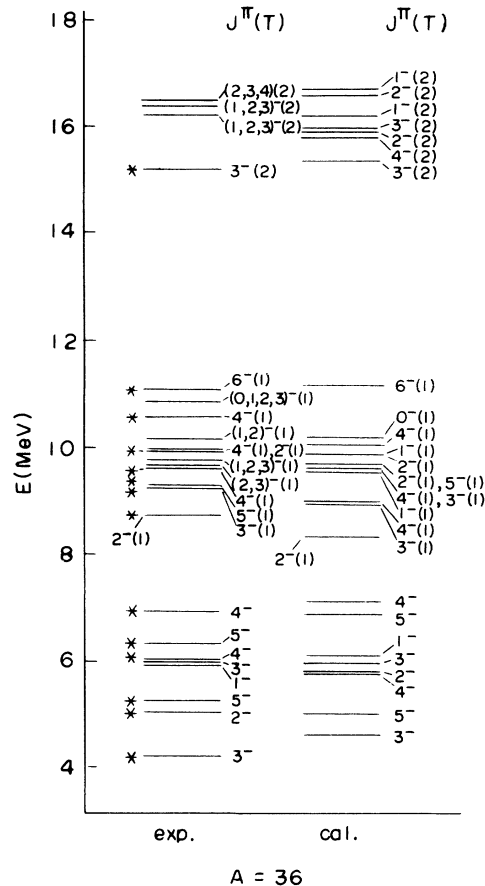


FIG. 5. Experimental and theoretical energy spectra for the $A=36$ nuclei.

square deviation. The only exception is the $A=40$ nuclei, which gives rms = 0.263 MeV for $T=0$, and 0.294 MeV for $T=1$.

Although we did not remove the spurious states due to the c.m. motion, the effect of the spurious states on the energy level calculation may still be negligible. The reason is as follows: The spurious states are distributed in the space with $1\hbar\omega$ excitation, and our model space contains only part of them. Furthermore, the intensities of the low-lying states are rather concentrated in some components of the basis states. Thus, the effect of spurious states is negligible, except in the calculation of energy levels of ^{40}Ca and $E1$ transition rates. For the two $T=0$, $J=1^-$ states of ^{40}Ca , the 1_1^- state contains 12% and the 1_2^- state contains 33% of the spurious state. For the other states in $A=36-39$, the effect of the spurious state is smaller than 10%.

B. Spectroscopic factors

Table II shows the spectroscopic factors of ^{40}Ca and ^{40}K for the $l=1$ and $l=3$ proton and neutron

TABLE II. The experimental and theoretical spectroscopic factors of ^{40}Ca and ^{40}K for the $l=1$ and $l=3$ stripping reactions on ^{39}K .

Nucleus	T	J_f^π	E_x^{exp} (MeV)	l	theo	exp ^a
^{40}Ca	0	3^-	3.74	3	0.42	0.49, 0.51, 0.60, 0.71
				1	0.25	0.01, 0.02
	0	5^-	4.49	3	1.00	0.65, 0.73, 0.76, 0.84, 1.22
	0	4^-	5.61	3	1.00	0.76, 0.78, 0.91, 1.31
	0	1^-	5.90	1	0.33	0.03, 0.05, 0.07
	0	2^-	6.03	3	0.99	0.19, 0.20, 0.22, 0.36
				1	0.01	0.04, 0.05, 0.06
	0	3^-	6.29	1	0.58	0.31, 0.40, 0.47, 0.61, 0.71
	0	3^-	6.58	1	0.16	0.11, 0.16, 0.17, 0.21, 0.23
	0	2^-	6.75	3	0.01	0.36, 0.50
				1	0.99	0.05, 0.19, 0.20
	1	4^-	7.66	3	0.96	0.60, 0.97, 1.22, 1.33
	1	3^-	7.69	3	0.90	0.79, 1.17
				1	0.05	0.06, <0.11
	1	2^-	8.42	3	0.86	0.56, 0.58, 0.64, 1.0
			1	0.08	0.02	
			3	1.00	0.69, 0.84, 0.91, 1.18	
^{40}K	1	4^-	0	3	0.96	0.90 ^b
	1	3^-	0.03	3	0.90	0.90 ^b
				1	0.05	0.02 ^b
	1	2^-	0.80	3	0.86	0.92 ^b
				3	0.08	0.02 ^b
			3	1.00	0.81 ^b	

^aReference 10.

^bReference 18.

stripping reactions on ^{39}K . For the $T=0$ states, we selected 8 levels with reliable J^π assignments. Among them, most of the states are in good agreement with the experimental ones. In general, the $T=1$ states are calculated better than those for $T=0$, especially for the neutron stripping reaction on ^{40}K , and this is consistent with the results obtained in the calculation on energy levels.

The spectroscopic factors of ^{39}K and ^{39}Ar for the $l=1$ and $l=3$ stripping reactions on ^{38}Ar listed in Table III. Our calculated values for this mass number agree very well with the observed ones. One state for which the agreement is not as good as the others is the $\frac{3}{2}^-$ state for $T=0$ at 3.02 MeV. The calculated value of 0.28 is overestimated compared to the observed value of 0.02. The level at 3.06 MeV of ^{39}Ar is tentatively assigned to $J^\pi = (\frac{5}{2}, \frac{7}{2})^-$; our calculated spectroscopic factor for the $\frac{1}{2}^-$ state agrees very well with the experiment.

Table IV presents the calculated and the observed spectroscopic information of ^{38}Ar and ^{38}Cl for the $l=1$ and $l=3$ stripping reactions on ^{37}Cl . The $l=3$ transitions for the 3_1^- , $T=1$ state at 3.81 MeV, the 3_1^+ , $T=2$ state at 0.76 MeV, and the 4_1^- , $T=2$ state at 1.31 MeV are all slightly underestimated. The $l=1$ transition for the 3^- , $T=2$ state at 0.76 MeV is overestimated. For the other states the agreements are very good. Maripuu *et al.*⁵ have calcu-

lated the spectroscopic factors of ^{38}Cl for neutron stripping in a larger model space. Our results are reasonably consistent with theirs.

Table V shows the spectroscopic information of

TABLE III. The experimental and theoretical spectroscopic factors of ^{39}K and ^{39}Ar for the $l=1$ and $l=3$ stripping reactions on ^{38}Ar .

Nucleus	T	J_f^π	E_x^{exp} (MeV)	l	theo	exp
^{39}K	$\frac{1}{2}$	$\frac{7}{2}^-$	2.81	3	0.82	0.60 ^a
	$\frac{1}{2}$	$\frac{3}{2}^-$	3.02	1	0.28	0.02 ^a
	$\frac{1}{2}$	$\frac{3}{2}^-$	4.08	1	0.53	0.30 ^a
^{39}Ar	$\frac{3}{2}$	$\frac{7}{2}^-$	0.0	3	0.73	0.60 ^b 0.66 ^c
	$\frac{3}{2}$	$\frac{3}{2}^-$	1.27	1	0.57	0.55 ^b 0.53 ^c
	$\frac{3}{2}$	$\frac{5}{2}^-$	2.09	3	0.00	0.01 ^b 0.02 ^c
	$\frac{3}{2}$	$\frac{3}{2}^-$	2.43	1	0.00	0.02 ^c
	$\frac{3}{2}$	$\frac{7}{2}^-$	2.48	3	0.15	0.09 ^b 0.07 ^c
	$\frac{3}{2}$	$\frac{3}{2}^-$	2.63	1	0.16	0.19 ^b 0.20 ^c
	$\frac{3}{2}$	$(\frac{5}{2}, \frac{7}{2})^-$	3.06	3	0.02	0.02 ^c

^aReference 19.

^bReference 20.

^cReference 21.

TABLE IV. The experimental and theoretical spectroscopic factors of ^{38}Ar and ^{38}Cl for the $l=1$ and $l=3$ stripping reactions on ^{37}Cl .

Nucleus	T	J_f^π	E_x^{exp} (MeV)	l	theo	exp
^{38}Ar	1	3^-	3.81	3	0.01	0.19 ^a
				1	0.06	0.01 ^a
	1	4^-	4.48	3	0.07	0.04 ^a
				3	0.37	0.34 ^a
1	5^-	4.59	3	0.32	0.31 ^a	
			1	0.01	0.01 ^a	
^{38}Cl	2	2^-	0.0	3	0.83	0.84 ^b 0.72 ^c
				1	0.01	0.02 ^c
	2	5^-	0.67	3	0.90	0.78 ^b 0.68 ^c
				1	0.27	0.09 ^b 0.08 ^c
	2	3^-	0.76	3	0.32	0.59 ^b 0.54 ^c
				1	0.27	0.09 ^b 0.08 ^c
	2	4^-	1.31	3	0.45	0.70 ^b 0.66 ^c
				3	0.05	
	2	3^-	1.62	1	0.20	0.40 ^b 0.29 ^c
				1	0.98	1.10 ^b 0.89 ^c
2	0^-	1.75	1	0.98	1.10 ^b 0.89 ^c	
			3	0.01		
2	2^-	1.98	3	0.01		
			1	0.43	0.70 ^b 0.48 ^c	

^a Reference 22.

^b Reference 23.

^c Reference 18.

TABLE V. The experimental and theoretical spectroscopic factors of ^{37}Ar and ^{37}Cl for the $l=1$ and $l=3$ stripping reactions on ^{36}Cl .

Nucleus	T	J_f^π	E_x^{exp} (MeV)	l	theo	exp
^{37}Ar	$\frac{1}{2}$	$\frac{7}{2}^-$	1.61	3	0.72	0.51 ^a 0.76 ^b
		$\frac{3}{2}^-$		1	0.60	0.35 ^a 0.44 ^b
	$\frac{1}{2}$	$\frac{3}{2}^-$	3.52	1	0.03	0.23 ^a 0.35 ^b
		$\frac{5}{2}^-$		3	0.00	0.03 ^a
	$\frac{1}{2}$	$\frac{1}{2}^-$	4.44	1	0.00	0.145 ^a 0.14 ^b
		$\frac{3}{2}^-$		1	0.02	0.02 ^a 0.01 ^b
^{37}Cl	$\frac{3}{2}$	$\frac{7}{2}^-$	3.10	3	0.13	
				1	0.06	
	$\frac{3}{2}$	$\frac{5}{2}^-$	3.71	3	0.46	
				1	0.03	
	$\frac{3}{2}$	$\frac{5}{2}^-$	3.74	3	0.12	
				1	0.03	
	$\frac{3}{2}$	$\frac{9}{2}^-$	4.01	3	0.01	
				3	0.86	
	$\frac{3}{2}$	$\frac{11}{2}^-$	4.55	3	0.86	
				3	0.00	
$\frac{3}{2}$	$\frac{13}{2}^-$	5.27	3	0.00		
			3	0.01		
$\frac{3}{2}$	$\frac{5}{2}^-$	5.38	3	0.01		
			1	0.10		

^a Reference 24.

^b Reference 25.

TABLE VI. The experimental and theoretical spectroscopic factors of ^{36}Ar and ^{36}Cl for the $l=1$ and $l=3$ stripping reactions on ^{35}Cl .

Nucleus	T	J_f^π	E_x^{exp} (MeV)	l	theo	exp
^{36}Ar	0	3^-	4.18	3	0.17	0.40 ^a
				1	0.30	0.06 ^a
	0	2^-	4.97	3	0.67	0.52 ^a
				1	0.02	0.02 ^a
	0	5^-	5.17	3	0.74	0.72 ^a
				0	1 ⁻	5.84
0	3^-	5.86	3	0.34	0.375 ^a	
			1	0.01		
^{36}Cl	1	2^-	1.95	3	0.74	0.86 ^b
				1	0.01	
	1	3^-	2.47	3	0.46	0.77 ^b
				1	0.11	0.10 ^b
	1	5^-	2.52	3	0.82	0.85 ^b
				1	0.26	0.45 ^b
1	$(2^-, 3^-)$	2.90	1	0.30	0.28 ^{b,c}	
			1	0.20	0.20 ^{b,d}	
1	2^-	3.21	1	0.10 ^b		

^a Reference 22.

^b Reference 26

^c For 2^- state.

^d For 3^- state.

^{37}Ar and ^{37}Cl for the $l=1$ and $l=3$ stripping reactions on ^{36}Cl . The calculated values for the $\frac{5}{2}^-$ state at 4.40 MeV and the $\frac{1}{2}^-$ state at 4.44 MeV for ^{37}Ar are zero. The experimental values for these two states are very small, however, these null results are due to the neglect of the $p_{1/2}$ and $f_{5/2}$ orbitals. Therefore, it may be more reliable to include these orbitals in the model space. The other states are in reasonable agreement with the observed ones. For ^{37}Cl the experimental results are not available. The spectroscopic information should be obtainable from the following suitable reactions: (d, p) or (t, d) on ^{36}Cl . Thus, we list also the predicted values of ^{37}Cl in Table V for future comparison. Since the two excitation levels for $J = \frac{5}{2}^-$ differ by only 0.03 MeV, the spectroscopic factors may be inverted.

The calculated and experimental spectroscopic factors of ^{36}Ar and ^{36}Cl for the $l=1$ and $l=3$ stripping reactions on ^{35}Cl are listed in Table VI. For the first 3^- state at 4.18 MeV of the nucleus ^{36}Ar , the agreement between the calculated and observed values is not as good as the others. The calculated values for most of the levels are in good agreement with the observed values with three exceptions: The $l=3$ stripping for the 2^- state at 1.95 MeV, the 3^- state at 2.47 MeV, and the 4^- state at 2.81 MeV of ^{36}Cl are slightly underestimated.

In conclusion, the agreements between our cal-

TABLE VII. The experimental and theoretical reduced width of EM transitions for nuclei of $A=36-40$.

Nucleus	J_i^π	E_{xi} (MeV)	J_f^π	E_{xf} (MeV)	Nucleus	J_i^π	E_{xi} (MeV)	J_f^π	E_{xf} (MeV)	Γ (10^{-n} eV)								
										exp ^a	theo	n						
⁴⁰ Ca	3 ⁻	3.74	0 ⁺	g.s.	³⁸ Ar	3 ⁻	3.81	0 ⁺	g.s.	5.9	1.4	6	E3					
	5 ⁻	4.49	3 ⁻	3.74		1.7	0.48	6	E2	4 ⁻	4.48	3 ⁻	3.81	3.0	61.3	4	M1	
	4 ⁻	5.61	3 ⁻	3.74		4.6	5.6	4	M1	5 ⁻	4.59	3 ⁻	3.81	3.5	4.3	7	E2	
						3.4	44.5	5	E2	4 ⁻	4.48	3.1	10.0	6	M1			
						1.3	1.1	4	M1	³⁸ Cl	3 ⁻	0.76	2 ⁻	g.s.	2.1	0.15	3	M1
						6.3	4.1	5	E2		4 ⁻	1.31	2 ⁻	g.s.	8.1	0.035	5	E2
	2 ⁻	6.03	3 ⁻	3.74		2.6	7.3	4	M1		5 ⁻	0.67	9.4	1.6	4	M1		
						2.0	0.013	3	E2		3 ⁻	0.76	2.2	0.017	4	M1		
	3 ⁻	6.29	5 ⁻	4.49		9.9	0.081	4	E2		3 ⁻	1.62	2 ⁻	g.s.	5.6	16.5	5	M1
	⁴⁰ K	3 ⁻	0.03	4 ⁻		g.s.	1.1	0.85	7	M1	5 ⁻	0.67	9.9	12.9	6	E2		
2 ⁻		0.80	3 ⁻	0.03	1.6	1.0	3	M1	3 ⁻	0.76	8.4	32.8	5	M1				
					<1.4	1.9	7	E2	4 ⁻	1.31	1.5	0.42	4	M1				
5 ⁻		0.89	4 ⁻	g.s.	5.4	12.8	4	M1	³⁷ Ar	3 ⁻	2.49	7 ⁻	1.61	5.7	1.6	5	E2	
					5.3	8.2	6	E2		9 ⁻	3.19	7 ⁻	1.61	1.6	5.3	3	M1	
³⁹ Ca	7 ⁻	2.80	3 ⁺	g.s.	1.2	3.7	7	E3					5.9	0.48	4	E2		
	³⁹ K	7 ⁻	2.81	3 ⁺	g.s.	2.7	5.1	7		E3	5 ⁻	3.27	7 ⁻	1.61	6.4	29.6	3	M1
		9 ⁻	3.60	3 ⁺	g.s.	6.2	0.10	6		E3				4.7	1.8	4	E2	
				2.81	4.6	50.4	6	M1	3 ⁻		2.49	1.2	1.4	3	M1			
				1.6	2.6	6	E2	3 ⁻	3.52	3 ⁻	2.49	3.1	1.4	3	M1			
				3.94	7 ⁻	2.81	3.2	1.0	5	E2	7 ⁻	3.53	7 ⁻	1.61	7.0	481.0	5	M1
				3.60	2.9	19.5	4	M1				6.8	0.82	4	E2			
				4.08	3.02	1.6	2.9	3	M1	9 ⁻		3.19	2.3	2.3	4	M1		
				4.13	2.81	1.5	0.63	2	M1	5 ⁻		3.27	4.5	26.8	5	M1		
				4.52	3.60	3.0	11.8	3	M1	11 ⁻	3.71	7 ⁻	1.61	1.5	0.49	3	E2	
				3.94	8.5	7.5	4	M1	9 ⁻		3.19	1.8	1.5	4	M1			
³⁹ Ar	5 ⁻	2.09	7 ⁻	g.s.	>1.1	14.2	3	M1	9 ⁻	4.02	7 ⁻	1.61	2.1	10.4	4	M1		
					>4.9	21.7	5	E2	9 ⁻		3.19	4.3	3.6	3	M1			
					1.27	5.1	11.6	4	M1	³⁷ Cl	7 ⁻	3.10	3 ⁺	g.s.	9.4	3.8	7	E3
					1.6	4.9	4	E2	9 ⁻		4.01	3 ⁺	g.s.	6.2	5.9	6	E3	
					1.27	4.7	16.5	4	M1					3.10	9.8	344.0	6	M1
				1.1	0.63	3	M1					4.0	1.6	6	E2			
				2.09	2.3	0.34	4	M1	11 ⁻		4.55	7 ⁻	3.10	<9.4	5.8	6	E2	
³⁹ Ar	3 ⁻	2.63	3 ⁻	1.27	3.8	265.0	5	M1	9 ⁻		4.01	1.9	1.4	4	M1			
					2.09	5.3	1.2	4	M1	13 ⁻	5.27	9 ⁻	4.01	<9.4	0.053	6	E2	
					1.9	2.8	3	M1	11 ⁻		4.55	1.9	10.3	4	M1			
					2.6	6.6	4	E2	³⁶ Ar	3 ⁻	4.18	0 ⁺	g.s.	1.3	0.23	5	E3	
					1.27	1.7	10.6	3		M1	2 ⁻	4.97	3 ⁻	4.18	1.7	6.2	5	M1
				>1.6	10.7	4	E2				2.0	0.062	5	E2				
									5 ⁻	5.17	2 ⁺	1.97	3.0	1.4	7	E3		

TABLE VII. (Continued)

Nucleus	J_i^π	E_{xi}	J_f^π	E_{xf}	Γ (10^{-n} eV)		n		Nucleus	J_i^π	E_{xi}	J_f^π	E_{xf}	Γ (10^{-n} eV)		n	
		(MeV)		(MeV)	exp ^a	theo					exp ^a		theo				
			3 ⁻	4.18	1.0	2.8	8	<i>E2</i>	³⁶ Cl					4.0	0.22	7	<i>E2</i>
	3 ⁻	5.86	3 ⁻	4.18	2.0	1.5	4	<i>M1</i>		5 ⁻	2.52	2 ⁺	g.s.	1.2	0.030	7	<i>E3</i>
	4 ⁻	5.90	3 ⁻	4.18	1.3	1.4	3	<i>M1</i>		4 ⁻	2.81	2 ⁻	1.95	1.6	415.0	9	<i>E2</i>
					3.3	4.0	5	<i>E2</i>				5 ⁻	2.52	6.3	12.6	5	<i>M1</i>
³⁶ Cl	3 ⁻	2.47	2 ⁻	1.95	4.5	3.5	4	<i>M1</i>						5.6	5.1	9	<i>E2</i>

^a References 10 and 27.

culated spectroscopic factors for the 3_1^- states of even-even nuclei with the observed ones are not as good as the other states with the exceptions of the $l=3$ stripping of ⁴⁰Ca and the $l=1$ stripping of ³⁶Cl. The overall results show that the calculated value for higher isospin states are, in general, better than those for lower isospin states. This fact manifests that our model space is more suitable for the higher isospin states. For lower isospin states, an enlarged model space is probably necessary.

C. Electromagnetic transition rates

We calculated *E2*, *E3*, and *M1* transition rates to provide a more sensitive test of the calculated complete wave functions. The reason we did not consider the *E1* transition rates is that the spurious states were not removed in the energy level calculation. Thus it would be meaningless to consider the *E1* transition rates. For electric multipole transitions, effective charges of $e_p = 1.5$ and $e_n = 0.5$ are assumed, which are consistent with the results obtained by Wilkinson,¹⁷ and the radial integrals are evaluated using harmonic oscillator wave functions, giving a total rms radius as determined from electron scattering with $\hbar\omega = 10.6$ MeV. The ground-state transitions in ³⁸Ar, ³⁷Cl, and ³⁶Ar are obtained with the wave functions of Sec. III A; for ⁴⁰Ca g. s., ³⁹Ca, and ³⁹K, a pure doubly closed shell-model state and a hole in $1d_{3/2}$ and $2s_{1/2}$ are taken. For *M1* transitions, the free gyromagnetic factors are used.

Table VII shows the calculated and experimental electromagnetic transition rates. The calculated results are in reasonably good agreement within a small factor for most of the transitions. For the electric multipole transitions, even we used large values of effective charges for the proton and neutron, most of the calculated results are still smaller than the experimental data. These discrepancies may be improved if an enlarged model space is assumed. For $A=39$ nuclei, we have

two *E3* transitions for ³⁹Ca and ³⁹K nuclei; the calculated results are all in reasonable agreement with the experimental ones.

For the *M1* transitions, much theoretical work has been performed previously.⁴⁻⁶ Our predictions are in uniformly good agreement with the observed values. In particular, the observed enhancement of the *M1* transition in ³⁸Cl between 3_2^- and 4_1^- , which cannot be accounted for by weak particle-hole admixtures, is predicted in reasonable agreement with the observed data in our model. For the other transitions, where comparison with previous works is possible, the agreement is also reasonable. Our calculated *M1* transition rates are slightly larger than the experimental data. This defect could probably be improved if the effective magnetic moments and a larger model space are taken into account.

D. Validity of the weak-coupling model

Ellis and Engeland²⁸ have formulated particle-hole states by coupling in *J* and *T* eigenfunctions resulting from diagonalization of $(sd)^{n_1}$ and p^{n_2} . The main assumption is that the correlations between particles in the same major shell are of predominant importance, and the p-h interaction can be treated as a small perturbation. The p-h states were selected by combining eigenfunctions obtained by solving the n_1 particle problem in the *sd* shell and the $12-n_2$ hole problem in the *p* shell. The negative-parity levels with $A=16-19$ were reproduced well with experiment.

In order to study how good the weak-coupling model is, we used our hole-hole interactions to calculate the wave functions for the low-lying positive-parity states within the $(d_{3/2}, s_{1/2})$ shells. These wave functions were then coupled by a particle in the $f_{7/2}$ or $p_{3/2}$ shell. The degree of the overlapping between these resultant wave functions and the wave functions for odd-parity states obtained in this work were then calculated. Our results show that the overlappings are about 90% or

TABLE VIII. Wave functions for the negative-parity states of ^{36}Ar and ^{36}Cl given in terms of the $(s_{1/2}, d_{3/2})^{n_1}$ and $p_{3/2}$ or $f_{7/2}$.

	T	J^π	$^{36}\text{Cl} (T=\frac{1}{2})$				$^{36}\text{S} (T=\frac{3}{2})$					Total	
			$\frac{3}{2}_1^+$	$\frac{1}{2}_1^+$	$\frac{5}{2}_1^+$	$\frac{7}{2}_1^+$	$\frac{3}{2}_2^+$	$\frac{5}{2}_2^+$	$\frac{3}{2}_1^+$	$\frac{1}{2}_1^+$	$\frac{5}{2}_1^+$		$\frac{3}{2}_2^+$
^{36}Ar	0	3_1^-	47	34	1	2	7	6					97
	0	2_1^-	69	1	14		2	11					97
	0	5_1^-	74		18	6		1					99
	0	1_1^-	32	31	8	3		24					98
	0	3_2^-	35		21		20	17					93
	0	4_1^-	16	1	52	2	14	6					91
	0	5_2^-	11		49	13	10	2					85
	^{36}Cl	1	2_1^-	75	4	6		5		7		1	
1		5_1^-	82		14	1					2		99
1		3_1^-	30	10	27	1	8		15	1	3	1	96
1		2_2^-	31	1	20		3	2	26	1	9	1	94

higher for most of the states except the $(T, J^\pi) = (\frac{3}{2}, \frac{5}{2}^-)$ and $(\frac{3}{2}, \frac{3}{2}^-)$ states for ^{37}Cl and $(0, 5_2^-)$ state for ^{36}Cl . The overlappings for all second excited states of each (T, J^π) decrease slightly. For illustration, Table VIII shows the overlappings between the non-normal parity state wave functions of $A=36$ and the wave functions obtained by combining the low-lying positive-parity state wave functions of $A=35$ and one nucleon in the $f_{7/2}$ or $p_{3/2}$ shell. The positive-parity levels of the $A=35$ nuclei are in the sequence of the experimental data. Our results show that it is reliable to apply the weak-coupling model to the calculation of negative-parity states of $A=35$ and 34 nuclei.

E. Effective interactions and two-body matrix elements

As mentioned in Sec. II, we have four interaction parameters $A_{0\text{hp}}$, $A_{1\text{hp}}$, $B_{0\text{hp}}$, and $B_{1\text{hp}}$ in the hole-

$$\begin{aligned} \epsilon(f_{7/2}) - \epsilon(d_{3/2}) = & \bar{\epsilon}(f_{7/2}) - \bar{\epsilon}(d_{3/2}) + \frac{1}{16} \sum_{T, J} (2T+1)(2J+1) \langle d_{3/2} f_{7/2} | V | d_{3/2} f_{7/2} \rangle_{TJ} \\ & - \frac{1}{4} \sum_{T, J} (2T+1)(2J+1) \langle d_{3/2}^2 | V | d_{3/2}^2 \rangle_{TJ}, \end{aligned}$$

where $\epsilon(j)$ and $\bar{\epsilon}(j)$ are the single-particle energies assuming ^{40}Ca and ^{32}S to be cores. After using the values of Erne for $\bar{\epsilon}(j)$ and two-body matrix elements, we get $\epsilon(f_{7/2}) - \epsilon(d_{3/2}) = 6.97$ MeV compared with 6.13 MeV for ours. Therefore, the consistency is satisfactory. In order to provide a more sensitive test of our calculated interaction

particle interaction, four parameters $A_{0\text{hh}}$, $A_{1\text{hh}}$, $B_{0\text{hh}}$, and $B_{1\text{hh}}$ in the hole-hole interaction, and three splittings of single-particle levels of $d_{3/2}$ - $s_{1/2}$, $f_{7/2}$ - $d_{3/2}$, and $p_{3/2}$ - $d_{3/2}$ to be determined in the least-squares fit. The searched values for these 11 parameters are -1.15 , -0.31 , -1.52 , 0.04 , -0.91 , -0.91 , -1.25 , 0.34 , 1.58 , 6.13 , and 7.93 MeV, respectively. The hole-hole interaction strengths have been used to reproduce the normal-parity ground states. The remarkable agreement between the calculated and observed ground state energies as shown in Table I indicates the reasonableness of the use of the modified surface- δ interaction.

In order to test the reasonableness of our single-particle level splittings, let us compare our results with those of Ern . To make the comparison possible, we have to make the following transformation:

strengths, we also calculated the two-body matrix elements for particle-particle and particle-hole. Table IX lists the two-body matrix elements in the $f_{7/2}$ and $d_{3/2}$ orbits. The values listed in the column entitled Ern  are those obtained by Ern  in his work of calculating the odd-parity levels with $A=33-41$. The column entitled MSDI contains the

TABLE IX. Two-body matrix elements in the $f_{7/2}$ and $d_{3/2}$ orbits.

T	J	Particle-particle (MeV)				Particle-hole (MeV)			
		Present	Erné	MSDI	G	Present	Erné	MSDI	G
0	2	-5.46	-3.65	-3.70	-3.62	-1.02	-1.85	-1.22	0.78
	3	-2.84	-1.85	-2.10	-1.90	-1.31	-2.87	-1.86	0.26
	4	-2.40	-1.77	-1.83	-0.87	-0.87	-1.18	-1.59	0.01
	5	-3.19	-2.90	-2.32	-2.21	-2.23	-1.92	-2.51	-0.94
1	2	0.04	0.38	0.70	-0.35	1.99	1.58	1.26	2.12
	3	-0.07	-0.08	0.54	-0.32	1.46	0.66	0.78	0.93
	4	0.04	0.92	0.70	-0.22	1.02	0.56	0.51	0.66
	5	-0.33	0.43	0.19	-1.11	2.22	1.35	1.22	1.62

results obtained by Glaudemans *et al.*²⁹ The data listed in the column G are those obtained by Osnes and Kuo.³⁰ The four sets are rather similar, except the $T=1$ matrix elements for particle-particle and $T=0$ matrix elements for particle-hole in column G have different signs from the other three sets. Our results for p-p are more attractive and those for p-h are more repulsive than those obtained by Ern e and Glaudemans *et al.* However, in general, our calculated two-body matrix elements for p-p and p-h in the $f_{7/2}$ and $d_{3/2}$ orbitals are reasonably consistent with the previous works.

IV. CONCLUSIONS

A modified surface-delta effective interaction has been used in a least-squares fit to energy level data of negative-parity states in the $A=36-40$ nuclei. The calculated energy spectra are in reasonable agreement with the observed values; the levels for odd-mass nuclei are in very good agreement with the experimental values. Some levels with model analogs, however, deviate by about 500 keV from the observed ones. This is probably due to the neglect of the other single-particle orbits.

Some very low-lying states contain large intensities of the components of $(f_{7/2}, s_{1/2}^{\pi_1})$, $(p_{3/2}, d_{3/2}^{\pi_2})$, $(f_{7/2}, s_{1/2}^{\pi_1}, d_{3/2}^{\pi_2})$, and $(p_{3/2}, s_{1/2}^{\pi_1}, d_{3/2}^{\pi_2})$ configurations. This seems to justify the necessity of the inclusion of the $s_{1/2}$ - and $p_{3/2}$ - orbits in the configuration space at least. The root-mean-square deviation for energy-level fitting in each mass number decreases as the mass number A increases for either the even mass nuclei or the odd mass nuclei. Higher isospin states, in general, give a smaller rms deviation for individual mass numbers. This fact shows the structure of higher isospin states may be simpler than that of lower isospin states and thus can be accounted for satisfactorily by our model space.

The spectroscopic factors are in good agreement with the experimental data. The $l=1$ and $l=3$ strippings for the 3_1^- state of even-even nuclei do not agree as well as the others. This discrepancy may be improved by taking into account the octupole vibration and/or the enlargement of model space.

The calculated EM transitions are in reasonable agreement with the observed values. Our calculated $E2$ and $E3$ transition rates are, in general, slightly underestimated. The predicted $M1$ transition rates, on the contrary, are slightly overestimated for most of the transitions. These discrepancies may be reduced, provided that an enlarged model space is taken into account and the effective magnetic moments are used.

We also tested the validity of the weak-coupling model by calculating the overlappings between the calculated wave functions for the non-normal parity states of mass number A in this work and the wave functions obtained by combining the low-lying positive-parity state wave functions with mass number $A-1$ and one nucleon in the $f_{7/2}$ - or the $p_{3/2}$ - shell. The wave functions for the low-lying positive-parity state are reproduced by the hole-hole interactions obtained in our calculation. Our results show that the degree of overlapping is larger than 90% for most of the states. This provides a suitable approach to study the structure of the nuclei for $A=34$ and 35 with the weak-coupling model.

In conclusion, the nuclear properties observed in the $A=36-40$ nuclei can be explained quite well by assuming a modified surface-delta type two-body interaction, provided that the model space is enlarged to include the $2s_{1/2}$, $1d_{3/2}$, $1f_{7/2}$, and $2p_{3/2}$ orbits.

ACKNOWLEDGMENT

This work was supported by the National Science Council of the Republic of China.

- ¹S. Goldstein and I. Talmi, *Phys. Rev.* **102**, 589 (1956).
²S. P. Pandya, *Phys. Rev.* **103**, 956 (1956).
³F. C. Ern , *Nucl. Phys.* **84**, 91 (1966).
⁴S. Maripuu and G. A. Hokken, *Nucl. Phys.* **A141**, 481 (1970).
⁵S. Maripuu, B. H. Wildenthal, and A. O. Ewwaraye, *Phys. Lett.* **43B**, 368 (1973).
⁶S. T. Hsieh, K. T. Kn pfle, and G. J. Wagner, *Nucl. Phys.* **A254**, 141 (1975).
⁷H. Hasper, *Phys. Rev. C* **19**, 1482 (1979).
⁸R. R. Scheerbaum, *Phys. Lett.* **61B**, 151 (1976).
⁹W. J. Gerace and A. M. Green, *Nucl. Phys.* **A113**, 641 (1968).
¹⁰P. M. Endt and C. van der Leun, *Nucl. Phys.* **A310**, 1 (1978).
¹¹P. Baumann, A. -M. Bergdolt, G. Bergdolt, A. Huck, G. Klotz, G. Walter, H. V. Klapdor, H. Fromm, and H. Willmes, *Phys. Rev. C* **18**, 2110 (1978).
¹²M. Sakakura, A. Arima, and T. Sebe, *Phys. Lett.* **61B**, 335 (1976).
¹³L. B. Hubbard and H. P. Jolly, *Phys. Rev.* **178**, 1783 (1969).
¹⁴W. A. Sterrenburg, G. Van Middelkoop, J. A. G. De Raedt, A. Holthuizen, and A. J. Rutten, *Nucl. Phys.* **A306**, 157 (1978).
¹⁵E. Sugarbaker, R. N. Boyd, D. Cline, P. B. Vold, J. R. Lien, and P. R. Goode, *Phys. Rev. C* **19**, 714 (1979).
¹⁶H. J. M. Aarts, G. A. P. Engelbertink, H. H. Eggenhuisen, and L. P. Ekstr m, *Nucl. Phys.* **A321**, 515 (1979).
¹⁷D. H. Wilkinson, *Comments Nucl. Part. Phys.* **1**, 139 (1967).
¹⁸C. L. Fink and J. P. Schiffer, *Nucl. Phys.* **A225**, 93 (1974).
¹⁹K. T. Kn pfle, P. Doll, G. Mairle, and G. J. Wagner, *Nucl. Phys.* **A233**, 317 (1974).
²⁰W. Fitz, R. Jahr, and R. Santo, *Nucl. Phys.* **A114**, 392 (1968).
²¹S. Sen, C. L. Hollas, C. W. Bjork, and P. J. Riley, *Phys. Rev. C* **5**, 1278 (1972).
²²M. A. Moinester and W. P. Alford, *Nucl. Phys.* **A145**, 143 (1970).
²³J. Rapaport and W. W. Buechner, *Nucl. Phys.* **83**, 80 (1966).
²⁴S. Sen, C. L. Hollas, and P. J. Riley, *Phys. Rev. C* **3**, 2314 (1971).
²⁵S. Sen, W. A. Yoh, and M. T. McEllistrem, *Phys. Rev. C* **10**, 105 (1974).
²⁶P. Decowski, *Nucl. Phys.* **A169**, 513 (1971); **A196**, 632 (1972) (Erratum).
²⁷P. M. Endt and C. van der Leun, *At. Data Nucl. Data Tables* **13**, 67 (1974).
²⁸P. J. Ellis and T. Engeland, *Nucl. Phys.* **A144**, 161 (1970).
²⁹P. W. M. Glaudemans, P. J. Brussaard, and B. H. Wildenthal, *Nucl. Phys.* **A102**, 593 (1967).
³⁰E. Osnes and T. T. S. Kuo, *Phys. Lett.* **47B**, 430 (1973).